

TRANSIENT PRESSURE WELL TEST ANALYSIS OF FRACTURED GEOTHERMAL WELLS

Hafeza A. Bakar* and Sadiq J. Zarrouk

Department of Engineering and Science, The University of Auckland, Private Bag 92019, Auckland, New Zealand

*habu538@aucklanduni.ac.nz

Keywords: *Transient pressure analysis, TOUGH2, PyTOUGH, water injection, geothermal wells, fractured wells.*

ABSTRACT

Fracturing during injectivity testing can take place in geothermal wells when the reservoir has a low permeability or when the well has skin damage. The transient behavior (pressure falloff) of these wells can't be matched using existing well test analysis methods. At the same time, modelling fracturing in geothermal reservoirs using rock mechanics and commercial finite element software is complicated due to several field uncertainties (e.g. formation height, reservoir permeability and porosity). In addition, rock mechanics data (rock stress, strain and Young's modulus), which are normally unknown in geothermal fields. This makes it difficult to develop an appropriate fracture model that matches the field test data.

This study attempts to develop a fracture model without integrating the rock mechanics. The model is setup with a simple grid using the TOUGH2 geothermal reservoir simulator and validated using the advanced pressure derivative transient analysis. Multiple subsets of fracture geometries were developed to represent the different stages of fracture closure during pressure falloff. The PyTOUGH code was used to simplify the running of the different fracture stages.

The results are very promising and provide a clear justification and explanation for the fractured well behavior. This model should be of use in matching data from geothermal wells with similar pressure response.

1. INTRODUCTION

Injection/falloff tests are commonly carried out upon completion of drilling geothermal wells. This is to obtain the wells injectivity, estimate the formation permeability, Skin and reservoir pressure.

During the water injection part of the test, it is possible that fracturing of reservoir rock occurs when the reservoir has low permeability or where there is skin damage near the well (Abou-Sayed et al., 1996; Clark, 1968; Nikraves et al., 1996). When this takes place, all existing (conventional) well test analyses techniques will fail to match reservoir pressure response. This is because fracture (rock) mechanics should be considered in the solution, while conventional well test analyses methods, do not account for them.

Well fracturing can take place when high-pressure fluid introduces into the reservoir (Fjaer et al., 2008; Hubbert and Willis, 1972; Yew and Weng, 2014). This behavior is known to drilling engineers as it can result in problems during cementing of deep well casings. This is because the fluid pressure within the rock exceeds the minimum

principal stress of the rock and causes splitting/fracture of the rock. Fractures form perpendicular to the least principal stresses. Thus, it can be vertical or horizontal fracture depending to the orientation of the least principal stress. For example in a reservoir with a depth approximately more than 1500m, vertical (z direction) fracture is likely to form as the least principal stress is likely in horizontal (x or y) direction (Ahmed, 2006; Hubbert and Willis, 1972). In some shallow formations on the other hand, least principal stress is usually the overburden (vertical) stress, thus fracture will propagate in horizontal direction (Ahmed, 2006; Hubbert and Willis, 1972).

Figure 1 presents the typical pressure behaviour of a fracture formation during an injectivity test. The breakdown pressure is the maximum pressure where the formation breaks down and initiates a fracture formation. The fracture propagates as the injection continues and at the same time fluid leaks off from the fracture to the surrounding rock. When the injection is ceased, a rapid pressure drop is observed due to no friction pressure loss to fluid flow in the fracture. The pressure at this point is called instantaneous shut-in pressure (ISIP). Fluid continues to leak off from the fracture into the formation and fracture opening decreases until the fracture closure. Then, the fluid pressure transient gradually and transitioning into pseudo-linear or radial flow.

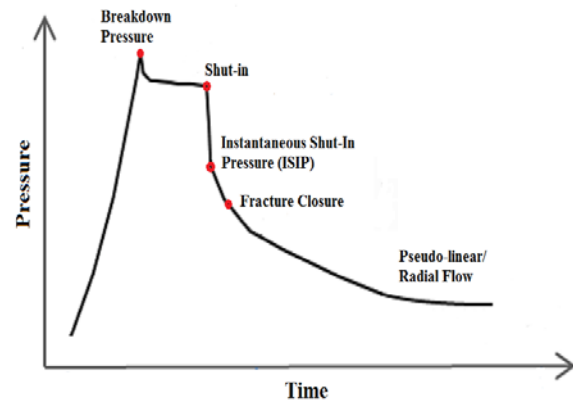


Figure 1: Pressure response of a fracture well during injection (after Hubbert and Willis, 1972).

Rock mechanics are commonly integrated with hydraulic mechanics for fracture modelling and it has been broadly implemented in commercial finite element software (Ingraffea and Heuze, 1980; Noorishad et al., 1982; Rutqvist et al., 2002). Many studies especially in oil and gas industry, have reported good results from the usage of the fracture model using this approach (Bai et al., 1999; Detournay, 2004; Jing et al., 2001). Nevertheless, this is not the case for

geothermal fields. Unlike oil and gas fields, geothermal fields have more uncertainties and limited information on rock mechanics. These uncertainties and unknowns can lead to poor matching with real field data.

In this work we will use numerical reservoir simulation to model the fracture behavior of such wells during pressure fall off using the TOUGH2 geothermal modeling software. TOUGH2 is a multipurpose numerical simulator, which was originally designed for geothermal reservoir and high-level nuclear waste storage problems (Pruess et al., 1999). It also has wider applications for solving other problems related to heat and mass transfers in porous media. This simulator used integral finite difference method to solve the numerical problem (Pruess et al., 1999). A python script was written to simplify the running of multiple models.

Prior to this study, parallel coupling between TOUGH2 and ABAQUS™ solid mechanics software was attempted to match the well test data from several geothermal wells. Unfortunately, the results were not satisfactory with poor data match between simulated and real data. This is likely due to unknown rock properties of the fields and limited self-control of some solution parameters in ABAQUS™ software.

The objective of this study is to develop a fracture model without explicit fracture mechanics modeling. The model is solely setup using geothermal reservoir simulator to explore the type, extent (length) and permeability of fracture. The result is then analysed and matched using advanced transient pressure analysis method for further data validation using well test data from the Soda Lake geothermal field, Nevada.

2. CASE STUDY: SODA LAKE GEOTHERMAL FIELD, NEVADA

2.1 Overview

Soda Lake geothermal field is located in the Carson Desert, west central Nevada (Figure 2). The first thermal waters were discovered in 1903 when a well drilled at the site of a hot spring northeast of Soda Lake encountered hot water at a depth of 18m (Sibbett, 1979).



Figure 2: The Soda Lake geothermal field location

Geothermal drilling activity began in the mid 1970s and still ongoing. Up to 2011 (McLachlan et al., 2011), there were more than 28 deep production, injection, observation and temperature gradient wells onsite. In addition, there are 70 others shallow water wells and survey drill-holes.

Soda Lake field has proved reserves of 20MWe and indicated resources of 41 MWe (McLachlan et al., 2011). There are two power-producing facilities in the field with a total capacity of 23MWe (Ohren et al., 2011). This field has been producing electricity since 1989 and currently operating at 16Mwe (McLachlan et al., 2011; Ohren et al., 2011).

2.2 Well-X

Well-X was drilled in 2009 to a depth of 2741m (Ohren et al., 2011). The casing depth of the well is 2122m and a liner was installed from 2122m to 2741m. The feed zone is found at depth of 1183m to 1186m. An injection falloff test was carried out on this well on January 2010, the pressure response during fall off at depth of 1184m and pressure derivative on log-log plot of the test are shown in Figure 3 and Figure 4 respectively. There is no recorded pressure of injection period prior to fall-off during this test. Deflagration process was carried out during September and December 2010 at the upper zone and shallow part of the well to improve the well performance. The well had produced an average of 0.044m³/s at 169°C since.

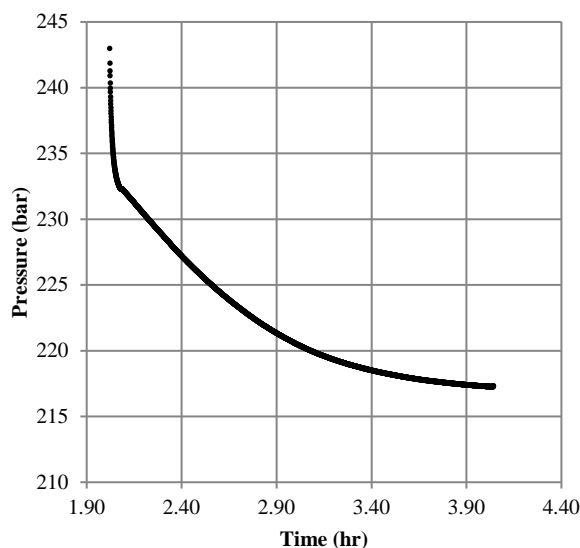


Figure 3: Pressure falloff response from an injectivity test for Well-X.

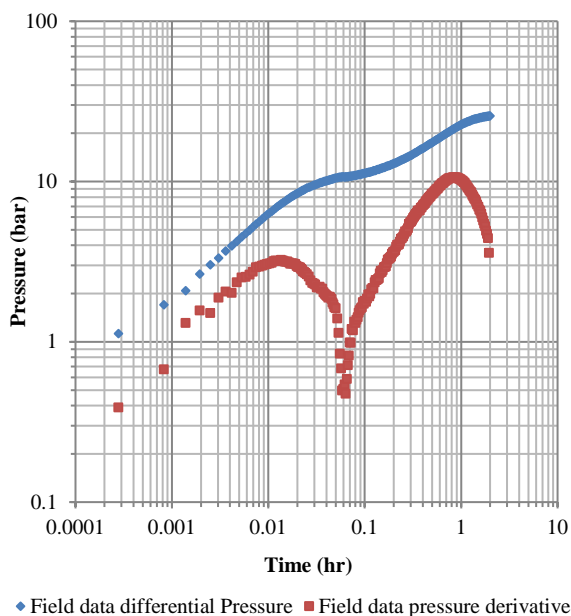


Figure 4: Pressure and pressure derivative plots of the falloff response of Well-X.

3. MODEL SETUP

The pressure falloff behavior of Well-X (Figure 3) is similar to that of Figure 1 indicating that fracturing took place during the injection test. Nonetheless, the type of fracture (vertical or horizontal) is unknown. Therefore, two numerical models of vertical and horizontal fractures were setup using the TOUGH2 simulator (Pruess et al., 1999) based on an injection test into Well-X condition in Soda Lake geothermal field, Nevada. A PyTOUGH script (Croucher, 2013) was written for automating the models running and data matching. The computation grid structures for both models are as shown in Figure 5 and Figure 6 respectively. The reservoir model input parameters for both models are given in Table 1. These input parameters were based on measured field data when possible, while the remaining parameters were either calculated or assumed.

The vertical fracture model (Figure 5) concept adapted a simple vertical fracture models (Perkins and Kern, 1961) such as Khristianovich-Geertsma-de Klerk (KGD) (Geertsma and De Klerk, 1969) and Perkins-Kern-Nordgren (PKN)(Nordgren, 1972). The minimum in-situ stress is in the horizontal plane and the vertical fracture plane is perpendicular to the minimum in-situ stress.

Meanwhile for horizontal fracture model (Figure 6), the concept was referred to penny-shaped (also known as pancake) fracture model (Abe et al., 1976; Perkins and Kern, 1961; Savitski and Detournay, 2002). The fracture becomes radial shape when the vertical distribution of minimum in-situ stress is uniform.

For both models, the width of a fracture is represented by the fracture block size. This can be seen in Figures 5-6 as red blocks. The width of the vertical and horizontal fractures is 12.5m and 0.01m respectively (Table 1). The fracture width remains constant throughout the simulation run, while the fracture half-length and radius changed were changed to match the field data.

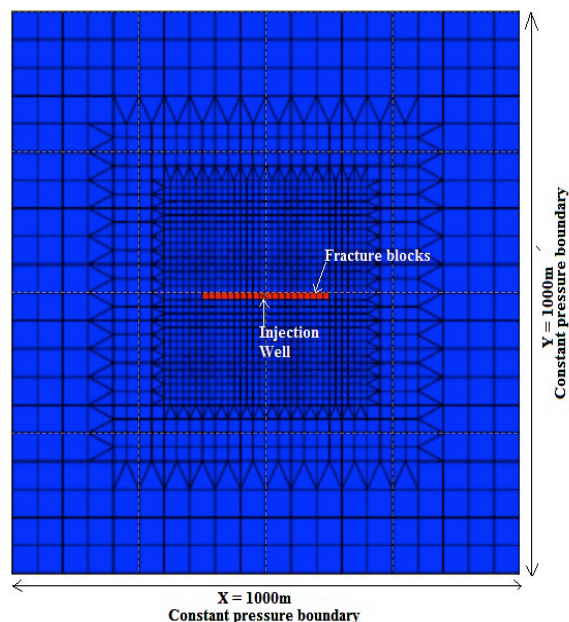


Figure 5: The modeling grid structure for the vertical fracture model.

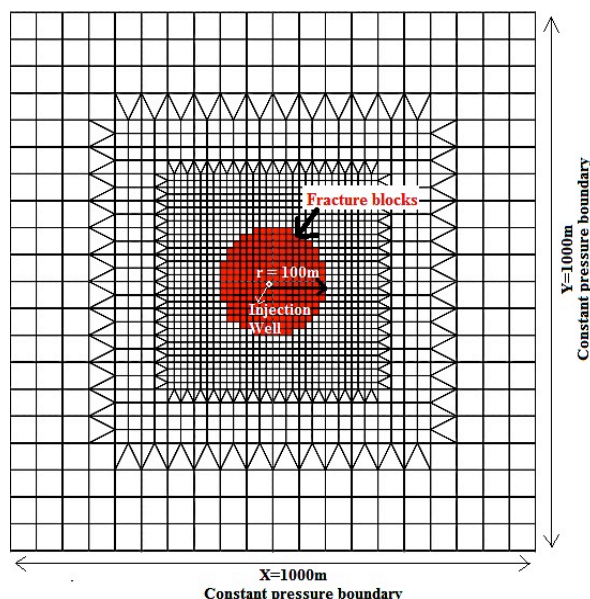


Figure 6: The modeling grid structure for the horizontal fracture model.

Table 1: Input parameters for the models

Parameter	Value	Unit (SI)
Fracture half-length	100 ^(a)	m
Fracture radius	100 ^(a)	m
Layer thickness	800 ^(m)	m
Vertical fracture thickness	800 ^(m)	m
Horizontal fracture thickness	0.01 ^(a)	m
Initial reservoir pressure	213 ^(a)	bar
Initial reservoir temperature	175 ^(m)	°C
Reservoir permeability	0.35 ^(c)	mD
Reservoir porosity	0.1 ^(a)	
Injection rate	7.57 ^(m)	kg/s

(a) Assumed data, (m) measured data, (c) calculated data

The following assumptions were made in this study:

- Symmetrical fracture growth from an injection point during pressure falloff.
- Only one fracture is used for each model
- The vertical fracture is a straight line.
- Homogenous reservoir rock.
- Isotropic rock matrix and permeability.
- The injection rate is constant during injection period.
- No attempt was made to investigate the fracture width in both models.

3. MODELLING RESULTS

Both vertical and horizontal fracture models were run for full injection and pressure fall-off period as shown in Figure 7 and 8 respectively. There are about twenty PyTOUGH runs of multiple models for each fracture model with changing fracture size and permeability to match the field data.

Overall, the optimized vertical fracture model gives a very good fit to the real pressure data as shown in Figure 7. The optimized horizontal fracture model meanwhile gave a satisfactory early behavior but poor match in the later time to the field data (Figure 8). Reasonable matching of the field data is observed at times between 1.94hr and 2.50hr, while poor data matched is found from time 2.50hr till 4.00hr. This indicates that vertical fracture propagation is more suitable compared to horizontal fracture design for this well. The difference in the results between vertical and horizontal fractures may also be caused by the grid used for each model. However, no attempt has been made to carry a mesh independence study at this stage.

This pressure response in Figures 7 and 8 were further analysed using the pressure difference and its derivative on the log-plot of both fracture models as shown in Figures 9 and 10. The pressure derivative result from the vertical fracture model (Figure 9) shows a satisfactory match with the field data in the early period (0.0001 to 0.1hr) and a good match in the later period (0.12 to 1.50hr). While the pressure derivative plots for horizontal fracture model (Figure 10), gave a relatively poor match to the field data.

It can be identified from Figures 9 and 10 that the field pressure derivative displays two humps and a sharp dip between those humps. The first hump represents the quick pressure drop while the fracture is open after injection ceases. The sharp dip meanwhile shows the fracture closing near the well. The later hump depicts normal pressure declining before reaching steady (infinite acting) reservoir pressure. The vertical fracture model pressure derivative (Figure 9) has shown close fit to the two humps. Yet the sharp dip has satisfactory match. On the other hand the horizontal fracture pressure (Figure 10), no clear hump is shown in the plots and the dip is very small. The field and model data match is also relatively poor.

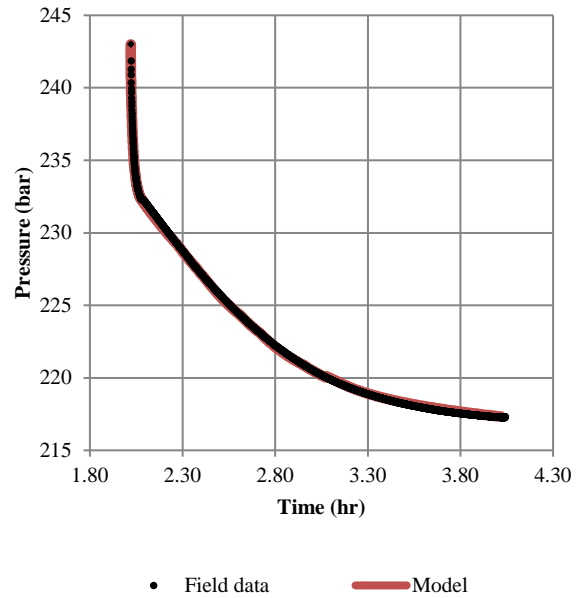


Figure 7: Fall-off pressure response between the vertical fracture model and field data (Well-X).

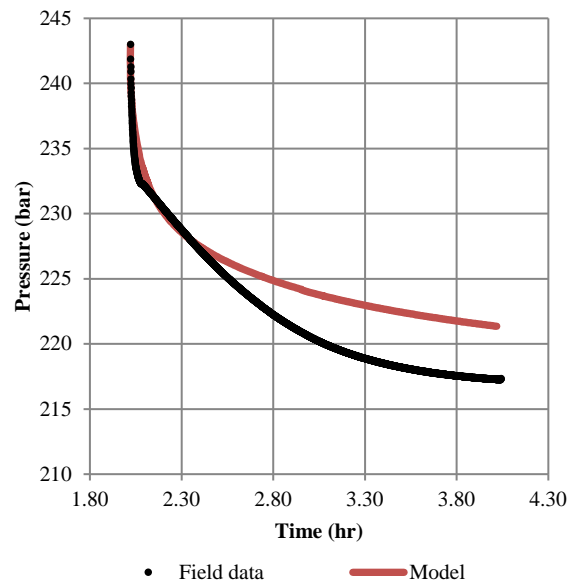


Figure 8: Fall-off pressure response for horizontal fracture model and field data (Well-X).

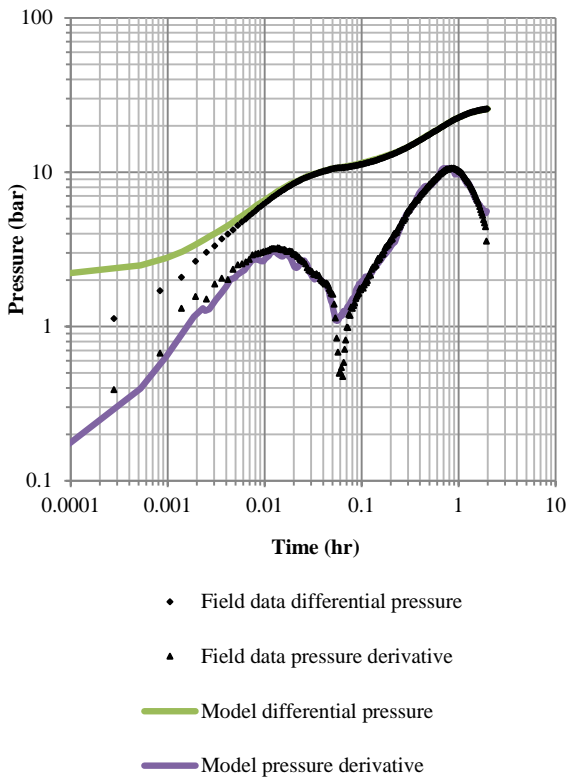


Figure 9: The pressure and pressure derivatives of vertical fracture model and field data on log-log plot.

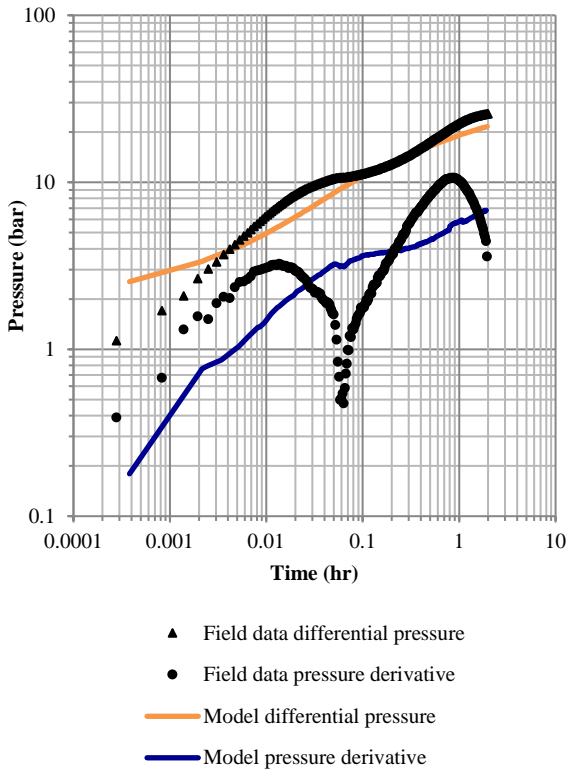


Figure 10: The pressure and pressure derivatives of horizontal fracture model and field data on log-log plot.

Figure 11 shows the fracture half-length and fracture permeability responses over time during fall-off for vertical fracture model. It is found that the fracture half-length and permeability decreases immediately after injection shut down till fracture closure at 2.08hr. After that, the fracture half-length as well as fracture permeability are found to gradually increasing until certain time and becomes constant eventually. The half-length discontinues growing at 2.72hr and the final fracture half-length is 25m. The fracture permeability meanwhile ceases from rising at 3.07hr with the final fracture permeability is 2.97 mD, which is an order of magnitude higher than matrix permeability. Fracture growth and fracture permeability increase may be due to the well damages and skin effects after fracture closure time.

Figure 12 on the other hand demonstrates the fracture radius length and fracture permeability over time for horizontal fracture model. Similar to Figure 11, the fracture radius/length and fracture permeability decreases over time until the fracture closes at 2.08hr. Then, fracture length is constant at 18m till the end time, while fracture permeability exhibits little increment at time 2.95hr.

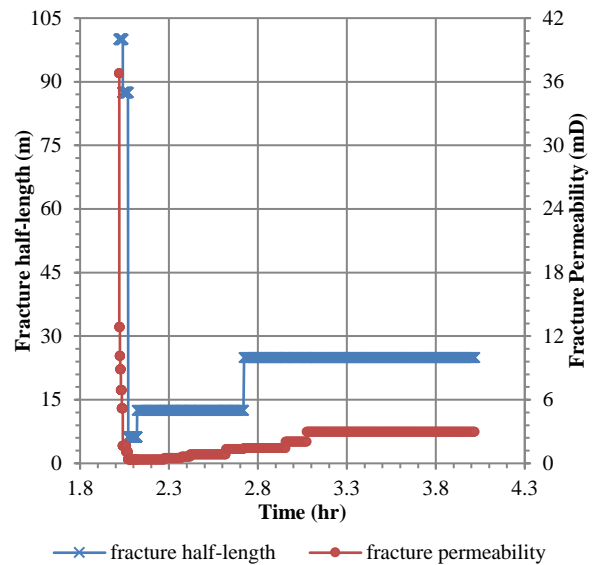


Figure 11: Fracture half-length, x_f and fracture permeability k_f over time for vertical fracture model of Figure 9.

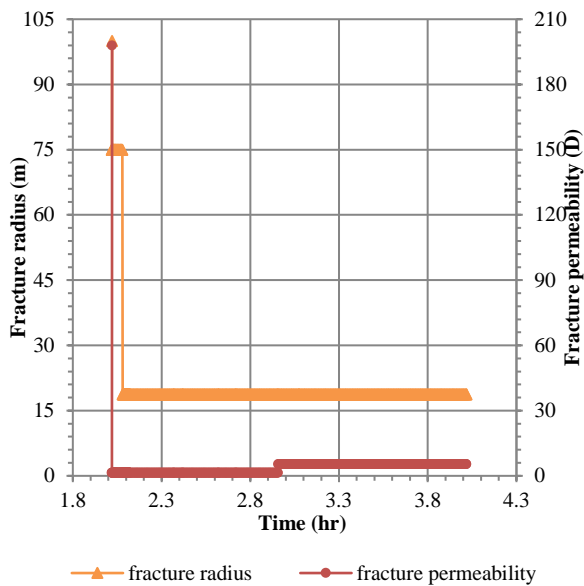


Figure 12: Fracture radius and fracture permeability over time for horizontal fracture model of Figure 10.

3.1 Geothermal wells with similar behaviour

There are several other reported geothermal wells that show similar pressure response after injection tests as shown above in Well-X. The wells are Well-Y from Soda Lake, Nevada and Well-Z from Wairakei, New Zealand. The pressure response and pressure derivative plots of these wells are presented in Figure 13 and Figure 14 respectively. The log-log plots shown in these figures were based on measured pressure data recorded during field injection (completion) testing.

There are two humps and a sharp dip in between found in the pressure derivative plots. These behaviors are similar to Well-X, which indicate a comparable fracture closure maybe taking place in these wells. However, the exact fracture orientation (vertical or horizontal) cannot be determined based on these data. This can only be determined after running multiple TOUGH2 models to this field data. The models for these wells are not discussed here and will be the subject of further work.

Interestingly, Figure 14 shows a further dip in pressure at much later times followed by pressure increase. Some events are likely to have taken place during that period such as another fracture formation due to other factors such as the closure of another feed zone. Or this could possibly be thermal effects within the well bore affecting the final stage of pressure falloff.

This change however is not investigated in this work and will be the subject of further study in the future.

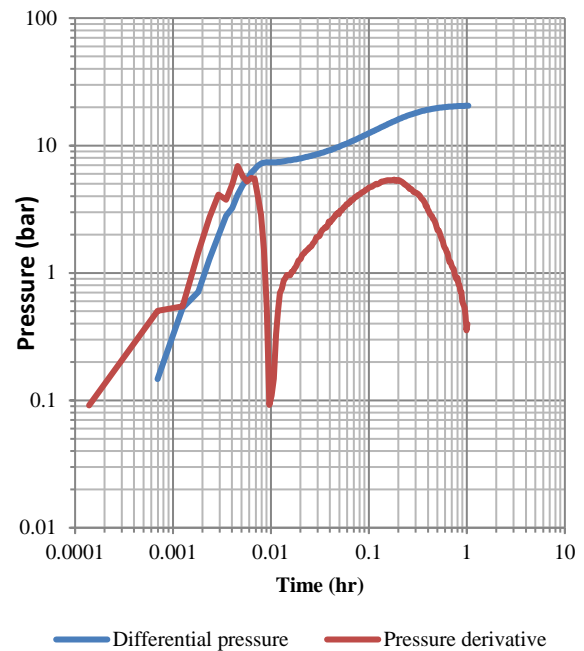


Figure 13: The log-log plot of pressure and pressure derivative for Well-Y

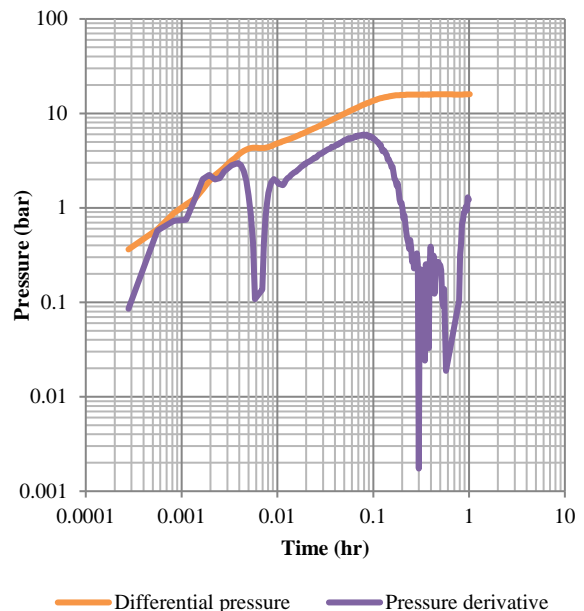


Figure 14: The log-log plot of pressure and pressure derivative for Well-Z

4. CONCLUSION

The following conclusions can be established from this study:

- The distinct drop in the pressure derivative during early pressure falloff is a clear indication of fracture closure.
- Unfortunately the early pressure response during reinjection is not available to us. Having this data

would have helped relate this analysis to the well injectivity and identifying the fracturing pressure.

- Vertical fracture model gives reasonably good match to the field data while the horizontal fracture model was not able to match Well X data. This indicates vertical fracture propagation during the testing of Well X.
- The method presented in this work simplifies well test analysis without including rock mechanics. It can be used to match field data of other fractured wells with similar pressure response (e.g. Wells Y and Z). This will allow the estimation of the reservoir permeability, fracture half-length, when conventional well test analysis is not successful.
- Fracture permeability plays an important role in matching the model and a field data.
- Fracture half-length and fracture permeability may increase after fracture closure due to factors such as wellbore damage or skin effect.
- It is possible that the later time dip in the pressure response seen in Well Z (Figure 14) is a result of more changes in the fracture behaviour. Further research is needed to investigate this behaviour.

ACKNOWLEDGEMENT

The authors would like to thank Mr. Ken Tyler from the University Nevada, Reno for providing the Soda Lake well test data and Mrs Katie Maclean of Contact Energy Ltd. for the Wairakei well data.

REFERENCES

- Abe, H., Keer, L., and Mura, T. (1976). Growth rate of a penny-shaped crack in hydraulic fracturing of rocks, 2. *Journal of Geophysical Research*, 81(35), 6292-6298.
- Abou-Sayed, I., Schueler, S., Ehrl, E., and Hendricks, W. (1996). Multiple hydraulic fracture stimulation in a deep horizontal tight gas well. *Journal of Petroleum Technology*, 48(02), 163-168.
- Ahmed, T. (2006). *Reservoir engineering handbook*: Gulf Professional Publishing.
- Bai, M., Meng, F., Elsworth, D., Abousleiman, Y., and Roegiers, J. C. (1999). Numerical modelling of coupled flow and deformation in fractured rock specimens. *International journal for numerical and analytical methods in geomechanics*, 23(2), 141-160.
- Clark, K. (1968). Transient pressure testing of fractured water injection wells. *Journal of Petroleum Technology*, 20(06), 639-643.
- Croucher, A. (2013). PyTOUGH user's guide, Department of Engineering Science, University of Auckland, Auckland, New Zealand.
- Detournay, E. (2004). Propagation regimes of fluid-driven fractures in impermeable rocks. *International Journal of Geomechanics*, 4(1), 35-45.
- Fjaer, E., Holt, R., Horsrud, P., Raaen, A., and Risnes, R. (2008). Mechanics of hydraulic fracturing. *Developments in Petroleum Science*, 53, 369-390.
- Geertsma, J., and De Klerk, F. (1969). A rapid method of predicting width and extent of hydraulically induced fractures. *Journal of Petroleum Technology*, 21(12), 1,571-571,581.
- Hubbert, M. K., and Willis, D. G. (1972). Mechanics of hydraulic fracturing.
- Ingraffea, A. R., and Heuze, F. E. (1980). Finite element models for rock fracture mechanics. *International Journal for Numerical and Analytical Methods in Geomechanics*, 4(1), 25-43.
- Jing, L., Ma, Y., and Fang, Z. (2001). Modeling of fluid flow and solid deformation for fractured rocks with discontinuous deformation analysis (DDA) method. *International Journal of Rock Mechanics and Mining Sciences*, 38(3), 343-355.
- McLachlan, H. S., Benoit, W. R., and Faulds, J. E. (2011). Structural Framework of the Soda Lake Geothermal Area, Churchill County, Nevada. *Geothermal Resource Council Transactions*, 35, 925 - 930.
- Nikraves, M., Kovscek, A., Johnston, R., and Patzek, T. (1996). *Prediction of formation damage during fluid injection into fractured, low permeability reservoirs via neural networks*. Paper presented at the SPE Formation Damage Control Symposium.
- Noorishad, J., Ayatollahi, M., and Witherspoon, P. (1982). *A finite-element method for coupled stress and fluid flow analysis in fractured rock masses*. Paper presented at the International Journal of Rock Mechanics and Mining Sciences & Geomechanics Abstracts.
- Nordgren, R. (1972). Propagation of a vertical hydraulic fracture. *Society of Petroleum Engineers Journal*, 12(04), 306-314.
- Ohren, M., Benoit, D., Kumataka, M., and Morrison, M. (2011). Permeability Recovery and Enhancements in the Soda Lake Geothermal Field, Fallon, Nevada. *Geothermal Resource Council Transactions*, 35, 493 - 497.
- Perkins, T., and Kern, L. (1961). Widths of hydraulic fractures. *Journal of Petroleum Technology*, 13(09), 937-949.
- Pruess, K., Oldenburg, C., and Moridis, G. (1999). TOUGH2 user's guide version 2. *Lawrence Berkeley National Laboratory*.
- Rutqvist, J., Wu, Y.-S., Tsang, C.-F., and Bodvarsson, G. (2002). A modeling approach for analysis of coupled multiphase fluid flow, heat transfer, and deformation in fractured porous rock. *International Journal of Rock Mechanics and Mining Sciences*, 39(4), 429-442.
- Savitski, A., and Detournay, E. (2002). Propagation of a penny-shaped fluid-driven fracture in an impermeable rock: asymptotic solutions. *International Journal of Solids and Structures*, 39(26), 6311-6337.
- Sibbett, B. S. (1979). Geology of the Soda Lake geothermal area, United States.
- Yew, C. H., and Weng, X. (2014). *Mechanics of hydraulic fracturing*: Gulf Professional Publishing.

